The International Archives of the Photogrammetry, Remote Sensing and Spatial Information Sciences, Volume XLVIII-5/W4-2025
Philippine Geomatics Symposium (PhilGEOS) 2025 "Enhancing Human Quality of Life through Geospatial Technologies",
24–25 November 2025, Quezon City, Philippines

Spatiotemporal Analysis of Mining-Induced Vegetation Loss in Homonhon Island Using Normalized Difference Vegetation Index: Possible Impacts on Biodiversity and Community

Margaux Angelica Cruz [1], Francesca Deighl Rivera [2]

[1] Department of Geodetic Engineering, University of the Philippines Diliman, Quezon City, Philippines - macruz4@up.edu.ph
[2] Philippine Space Agency, Quezon City, Philippines - fdrrivera1@gmail.com

Keywords: Mining, NDVI, Change Detection, Biodiversity, Deforestation, Sustainability.

Abstract

Homonhon Island in Guiuan, Eastern Samar is a historically and ecologically important site that has been subject to mining operations since the 1980s. Being rich in nickel and chromite, there are currently five mineral production sharing agreements in the 104 km^2 island inhabited by almost 5,000 residents. It is reported to be home to the critically endangered and endemic Philippine cockatoo, plus 72 endemic and 15 threatened plant species based on recent surveys. The almost 50 years of mining in the island resulted in lack of clean water and electricity, dust and noise pollution, reduction of crop yield and fisheries, deforestation, and threat to biodiversity. These alarming effects not only threaten the existence of the island and its current residents, but also pose a serious risk to the future generations. The evolution of the landscape due to the rampant mining activities were analyzed using NDVI on a time series of Landsat images from 1973 to 2024. The results show that about 56% of the land area exhibited overall NDVI decline, implying vegetation degradation or loss. The spatial overlay of the NDVI change results, building polygons, and threatened species illustrates the possible effects of mining areas on humans and biodiversity. The existence of mining tenements in more than 80% of the entire island poses serious threats, necessitating effective and comprehensive action. Geospatial technologies can provide a reliable means of monitoring mining areas, from planning to rehabilitation, to ensure compliance and help mitigate adverse impacts.

1. Introduction

1.1 Background

Mining is defined by the ISO as *"including exploration, opening-up, development, working of mineral deposits, drilling, construction of mines, mining operations, processing of minerals, etc."*. According to the World Mining Data by Reichl and Schatz (2022), global mining production dramatically increased by 52% from 2000 to 2020. The mining sector has its pros and cons, and is beset with controversy and differing views (Conde and Le Billon, 2017; Schoderer and Ott, 2022). Although it is a significant source of economic development, employment opportunities, and foreign trade, various studies have also associated mining with environmental and social impacts.

Heavy metals and trace elements from mining can contaminate the air, soil or water, affecting human health and the environment (Gupta et al. 2019; Prasad et al. 2021). These pollutants cause various types of human respiratory and gastrointestinal problems, organ failure, blood toxicity, skin diseases, deformities, and other disorders (Genchi et al. 2020). The expansion of surface mining can also lead to displacement of local communities, including indigenous peoples (Electronics Watch, 2022). There are also increased risks to human life due to mining accidents and higher exposure to natural hazards such as landslides and flooding (Ramadhan, 2023; Senouci, 2020). Many have reported that the mining sector is also surrounded by pressing issues such as corruption and human rights violations.

Land conversion and deforestation resulting from anthropogenic activities such as mining can impact biodiversity by causing habitat fragmentation, degradation, or loss. Forests are being cleared to make way for excavation pits, processing and storage sites, access roads, and worker settlement areas. A World Resources Institute article (Stanimirova et al. 2024) reported that mining activities around the world have increasingly encroached into tropical forests and protected areas. Moreover, studies have shown that mines and mineral deposits are spatially concentrated in high biodiversity areas (Murguía et al. 2016). Contamination of freshwater and marine ecosystems due to extensive mining impacts not only the aquatic biodiversity, but also the humans who consume these resources (Jitar et al. 2015). Leaching of pollutants into the soil can make it unsuitable for growth of vegetation (Dehkordi, 2024). Biodiversity and the natural environment in general, is a crucial aspect of human life due to the ecosystem services they provide. These benefits, which include sustenance, protection, health, livelihood, fuel, and shelter among others, support humans and affect the level of their well-being (Larsen et al. 2012; Zhang et al. 2019).

Small-scale gold mining activities in the Philippines was said to have started as early as the 3rd century, with gold trading increasing during the 12th to 14th century. The colonial period marked the start of commercial mining in the country. The Mines and Geosciences Bureau (MGB) under the Department of Environment and Natural Resources (DENR) is directly in charge of the administration and disposition of mineral lands and mineral resources, as well as the implementation of the Philippine Mining Act of 1995. The MGB estimated the mineral production value of gold, nickel ore, mixed nickel-cobalt sulfide, scandium oxalate, chromite, and iron at ₱132.69 billion in the year 2020. A 2023 report by Austrade mentions nickel ore and chromite as among the mined metals in the country, with operating mines corresponding to 59% and 7% out of the total operating mines as of 2022. Together with gold and copper, nickel ore and nickel products are among the country's top mineral exports according to the MGB. With 13% of global nickel production as of 2020, the country is the second top producer after Indonesia.

1.2 Objectives, Scope, and Significance

Mining is a temporary land use since mineral resources are finite (Williams, 2016). After mine closure, rehabilitation, health and safety, and sustainable land use measures must be implemented (Chugh et al. 2023; Peck et al. 2006). The Mines and Geosciences

Bureau of the Philippines (2025) mandates environmental protection throughout and after mining operations. Policies should ensure that mining benefits communities without compromising future generations. In line with the Convention on Biological Diversity, restoring degraded mining lands is vital to recover forest biodiversity and sustain ecosystem services. Despite existing monitoring policies, enforcement is limited by spatial and temporal constraints. Traditional site-level assessments often miss the broader impacts of mining on biodiversity (Sonter et al. 2018), and conservation efforts struggle to keep pace with rapid landscape changes. Spatial analysis offers a way to address these challenges. Homonhon Island, despite 50 years of intensive mining and related controversies, remains largely unexplored in geospatial research, with most studies focusing on ecology and biodiversity.

The general objective of this research is to add to the currently lacking geospatial work on the island. This study aimed to quickly identify the spatial distribution of the open pit mining areas in Homonhon Island by applying NDVI analysis on a series of Landsat images. Using the NDVI results from the 1970s to the 2020s, the two levels of analysis were applied to assess landscape changes due to mining activities. The NDVI change based on the general NDVI analysis aimed to inspect transitions from natural landscape to mined areas in the entire island, with particular focus on habitat degradation or loss. Furthermore, an initial exploration of the possible impacts of the mining-driven landscape change on the human population and threatened biodiversity were also done in combination with other spatial datasets.

2. Methodology

2.1 Study Area

The Philippines is among the 17 megadiverse countries, which together hold more than 70% of the world's biodiversity. However, the Philippines is also one of the world's 36 biodiversity hotspots, with high species endemicity but with only a small portion of original vegetation intact. Located in the west of the Philippines at 10°45′20″N, 125°44′21″E is the 104 km^2 Homonhon Island, in Guiuan, Eastern Samar (Figure 1). It is composed of eight barangays with a total human population of almost 5,000. Co-existing with the human communities in the island are a number of important species, including the endemic and critically endangered Philippine cockatoo (*Cacatua haematuropygia*) (Marticio, 2021). Recent floristic surveys within the island's ultramafic forests showcased its high floral biodiversity and endemism, with 72 endemic plant species and 29 threatened species according to the DAO-2017-11 (Romeroso et al. 2024). After a validation process in 2019, the DENR Region 8 recommended that the entire island of Homonhon be designated as a Critical Habitat. Adjacent to the island's eastern coastline is the Guiuan Protected Landscape and Seascape, a designated protected area rich in marine and coastal biodiversity.

Homonhon Island is known to have vast deposits of nickel and chromite, with exploratory works during the 1970s leading to the discovery of high chromite content. Large-scale mining operations in the island started in the 1980s, mainly for chromite extraction. There are currently five active mineral production sharing agreements (MPSA) and one application for exploration permit in the island. Locals mention that 60% of the island's land area has been denuded by mining operations. This is corroborated by digitized polygons from the May 2025 MGB Mining Tenement Control Map, showing MPSAs covering almost 63 km^2 or 60% of the total land area. There is also 3 km^2 or 3% of the island managed by the Philippine Mining Development Corporation (PMDC), the government's mining arm. In addition, there is one application for exploration permit (EXPA) covering almost 21 km^2 or 20% of the total area.

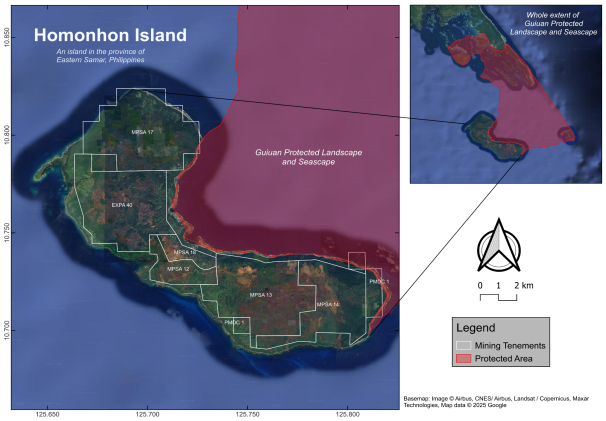

Figure 1. Homonhon Island with active mining tenements.

2.2 Data

Landsat images spanning 50 years were used in analyzing land cover change in Homonhon. Useful scenes, those with minimal cloud cover and free from data artifacts, were selected and downloaded using Google Earth Engine (GEE) and USGS EarthExplorer. Aside from cloud cover, which influenced the selection of image years to be used, the significant mining years in the island were also considered in image selection for the general change analysis. These significant years were based on the visible vegetation loss in the available satellite images due to the progression of mining activities in the island. Initial assessment indicated that the island was generally covered with vegetation prior to 1980, thus the use of 1970s satellite data as the "pre-mining" images. The several decades of active mining activities was investigated using post-1980s images, specifically from the 1990s onwards. There were no available usable images for the 1980s so these were not represented in the analysis.

To assess the general state of the land prior to the onset of mining activities, two 60-meter resolution Landsat 1 MSS images acquired on 06 January 1973 and 24 January 1973 were used as the baseline images. Landsat 8 images dated 13 April 2013 and 29 April 2013 were used as the intermediate images. Finally, the most recent image used in this analysis was a Landsat 8 image acquired on 31 August 2023. The Landsat MSS scenes were Tier 2 Level 1 Precision Terrain processing level, while the rest of the Landsat scenes used were in Tier 1 Level 2 Surface Reflectance processing level. These scenes downloaded from USGS EarthExplorer were originally in WGS 84 UTM Zone 52. The GEE images, meanwhile, were exported using the EPSG:32651 projection, WGS 84 UTM Zone 51. Additional years, consisting of 17 composite images from 1973 to 2024, were also processed in GEE to have a finer-scale perspective of the NDVI transition in the area. Although it is ideal to use images from the same season, cloud cover is a challenge for tropical countries. This was mitigated by using multiple images for some years to minimize unusable pixels (Table 1).

Collection	Year	Number of Images/Year
Landsat 1	1973	1
Landsat 2	1976, 1979	1, 2
Landsat 5	1995, 1997	1, 1
Landsat 7	2000, 2001	1, 2

Landsat 8	2013, 2015, 2016, 2017, 2018, 2019, 2021, 2022, 2023, 2024	2, 1, 2, 2, 1 2, 1, 2, 2, 2

Table 1. Year, number, and Landsat collection of images used.

The May 2025 version of the Mining Tenements Control Map was downloaded from the MGB Region 8 website. Administrative boundary shapefiles, based on the Philippine Statistics Authority (PSA) and National Mapping and Resource Information Authority (NAMRIA), were downloaded from the Humanitarian Data Exchange (HDX) under the United Nations Office for the Coordination of Human Affairs (OCHA). The extent of human population was quantified using the building shapefiles from OpenStreetMap (OSM) downloaded from Geofabrik GmbH's free download server. Since the OSM attribute data did not differentiate between mine camps or structures built for mining and the local community structures, all building polygons were used in the analysis. The extent of threatened species was represented using the known range of species downloaded from the IUCN Global List of Threatened Species. Records of threatened species in sampling sites from a recent survey (Romeroso et al. 2024) were also used as input.

2.3 Workflow

The methodology (Figure 2) used for two analysis levels, from data preparation, processing, detecting landscape change, and spatial analysis are described in the following subsections.

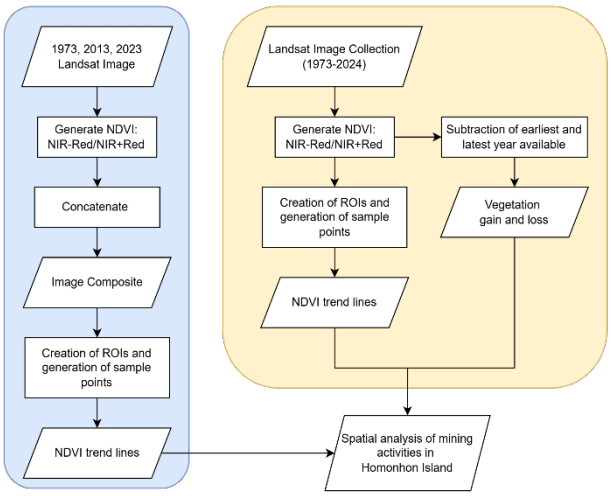

Figure 2. Workflow using ArcGIS Pro (blue) and GEE (yellow), from creation of NDVI images, NDVI change, and spatial analysis of possible mining impacts.

2.3.1 Image Preprocessing: Since the satellite images used were from different collections, dates, and processing levels, it was necessary to preprocess the data prior to further analysis. In particular, there are inherent challenges in using Landsat MSS images together with the other more recent Landsat series like Landsat 8 (Zhao et al. 2022). This was evident in the misalignment of the images and difference in spectral band coverage. Although the 2013 and 2023 Landsat 8 images had good alignment, the two 1973 images were severely misaligned with respect to the Landsat 8 images and to each other. To address this issue, image-to-image registration was performed on each of the two 1973 images using the 31 August 2023 image as the reference image. The Landsat MSS products have different spectral band ranges compared to more recent Landsat products, All Landsat images were clipped to Homonhon Island prior to further processing.

The images collected in GEE were carefully curated by prioritizing scenes with minimal cloud cover to ensure consistency and reliability in the vegetation index across time. A geometry was defined to automatically delineate the area of interest, serving as a spatial boundary for clipping the satellite imagery to the specified region. For years with multiple available images, the mean of the images was calculated and was used for processing. The QA_PIXEL band was utilized to mask out clouds and cloud shadows. It should be noted, however, that the readily-available QA band has its inherent limitations in completely removing all the unwanted pixels from the images. The dataset utilized atmospherically corrected surface reflectance imagery.

2.3.2 NDVI and Change Detection: The use of different Landsat sensors with Normalized Difference Vegetation Index (NDVI) has been effectively utilized in vegetation loss analysis (Markogianni and Dimitriou, 2016). Specifically, its usefulness in monitoring mining areas has been proven in other study areas (Li et al. 2015; Hengkai et al. 2020). Negative or very low positive NDVI values denote the absence of vegetation, and the value increases as the presence of vegetation becomes denser (Pettorelli, 2013). NDVI values of negative to 0.2 commonly denote non-vegetated areas such as cloud, shadow, water, rock, and bare soil. Moderate values of 0.2 to 0.5 typically represent sparse vegetation such as sparse trees and shrubs, grass, and croplands. High NDVI values of around 0.6 to 0.9 correspond to dense vegetation such as forests, dense trees, and crops at the peak of growth. Some adjustment in the NDVI ranges for identified classes in this study was used, since lower NDVI values were generally observed for tree cover, ranging from 0.4 to 0.5. These characteristics were used in identifying land cover changes and vegetation loss in particular, and to eliminate unwanted pixels such as clouds and shadows.

The NDVI images for each of the 1973, 2013, and 2023 Landsat scenes was generated using the NDVI raster function in ArcGIS Pro 3.4. For the Landsat MSS images, the NIR2 band was used in the NDVI computation due to lower between-sensor difference with newer Landsat products (Chen et al. 2019). The NDVI results for two scenes with the same acquisition year were then concatenated in the Raster Calculator to come up with a single cloud-free NDVI map for that year. The rationale for using this formula is that the NDVI values of clouds and cloud shadows are in the lower range or near zero, compared to the landscape pixels which are expected to have higher values. For each overlapping pixel from the image pair, this formula selects the pixel with the higher NDVI value and retains it for the resulting image (Eq. 1).

$$Con("[ndvi_1]" > "[ndvi_2]", "[ndvi_1]", "[ndvi_2]") \quad (1)$$

where $ndvi_1$ = NDVI map of scene 1 of the same year
$ndvi_2$ = NDVI map of scene 2 of the same year

A 3-year change map was then created by compositing the concatenated NDVI maps for each time period. Creating a 1973-2013-2023 RGB composite image displayed certain areas on the island with different colors, which were hypothesized to correspond to different change types. Regions of interests (ROIs) were drawn for all the identified change types and line graphs were generated using 100 sampling points for each class. The shape of these NDVI trend lines served as the basis for identifying the change types in the study area.

The ee.Image.normalizedDifference function in GEE was applied to compute the 17-year NDVI maps. The spectral bands used in the NDVI computation varied depending on the satellite mission, as different Landsat sensors were utilized throughout the

analysis. Bands 7 (NIR2) and 5 (Red) were used for the Landsat 1–2 MSS images, bands 4 (NIR) and 3 (Red) for Landsat 5 and 7, and bands 5 (NIR) and 4 (Red) for Landsat 8. A targeted set of points (Figure 3) representing visually decreasing or fluctuating NDVI values were selected to plot the 17-year NDVI change. White areas indicating NoData values, primarily due to cloud cover, were avoided. In addition, the spectral signatures corresponding to these point locations were analyzed to support the interpretation of vegetation dynamics and detect shifts in land cover characteristics. Areas exhibiting significant signs of vegetation degradation were cross-referenced with publicly available mining data.

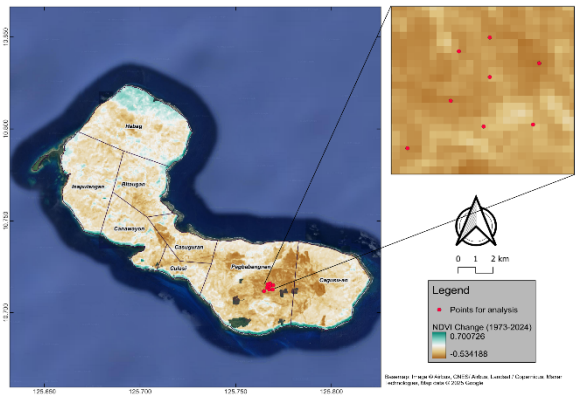

Figure 3. Eight randomly selected points used in the 17-year temporal plot of NDVI change.

A quantitative assessment of accuracy was established for the more recent NDVI results, particularly the 2023 and 2024 NDVI, using high-resolution Google Earth images as reference. A total of 2,800 points (Figure 4) were randomly generated within delineated validation polygons for bare area, grassland, and tree cover. It was ensured that these validation polygons did not overlap with the ROIs previously drawn for identifying the 3-year NDVI change types. A confusion matrix, with overall accuracy and kappa statistic, was generated in ArcGIS Pro for both NDVI results.

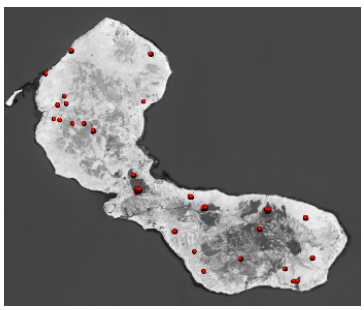

Figure 4. Accuracy assessment validation points overlaid on the 2023 NDVI image.

2.3.3 Spatiotemporal Impact Analysis: The Mining Tenements Control Map was georeferenced using the 2023 Landsat 8 image. This was used as the basemap for digitizing the Mineral Production Sharing Agreement (MPSA) and Application for Exploration Permit (EXPA) boundaries. The mining tenements shapefile was then overlaid with the NDVI change results to show which transitions occurred within the polygons, thereby showing where and when the mining-driven land cover changes occurred. These tenement boundaries were also used as the extent for computing areas and percentages of mined areas within approved sites.

The possible effect of these mining sites on the current human and threatened biodiversity population in the island were explored using spatial overlays of available datasets. The Select by Location tool was used to generate the number of OSM building features within the mining tenements. The sampling sites map from Romeroso et al. (2024) was georeferenced to digitize the location of sampling sites. Out of their list of threatened plant species, only those within the digitized mining tenements were included in the analysis. It should be noted, however, that there may be minor locational errors in the digitization of mining tenement polygons and sampling sites. As additional information for possible locations of threatened species, the IUCN Red List polygon shapefiles were intersected with the Homonhon Island polygon to extract the known range of threatened species.

3. Results and Discussion

The NDVI analysis was done at a general 3-year scale and a finer 17-year scale. The results from these two levels of analysis were compared to check for consistency and assess the applicability of each method.

3.1.1 NDVI and Change Detection: The 1973 and 2013 image subsets and the corresponding concatenated NDVI results are shown in Figure 5. These concatenated NDVI results for 1973 and 2013, plus the single NDVI result for 2023, were used in the 3-year general change analysis.

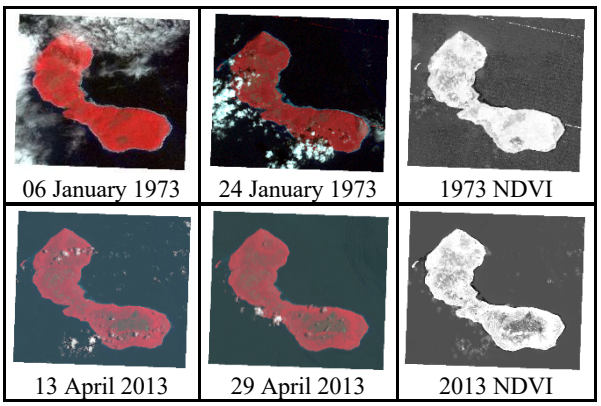

Figure 5. False color image subsets and corresponding concatenated NDVI results.

It is evident from this side-by-side visualization that the effect of haze, clouds, and cloud shadows were eliminated for almost all the pixels in the final NDVI results. This process was a quick and simple approach in removing those image features compared to using the Landsat QA band, which did not completely mask out the unwanted pixels. One limitation of this technique was that an image pair acquired within a few days should be used to eliminate effects of seasonality and land cover change. Moreover, when the image pair has unwanted pixels that overlap, which occurred for a small area in the northwest portion of the 1973 images, the combined NDVI for those areas will still have low values. Bright pixels due to artifacts will also not be eliminated using this technique, as was the case for the second Landsat MSS image.

The 3-year change map resulting from the image composite of concatenated NDVI maps is shown in Figure 6. Using the image composite, various temporal variations were easily identifiable based on their colored appearance on the image. The most glaring finding based on this image is the large red area (Class 1) in the southwestern part of the island within MPSA 13 and 14, indicating the shift from tree cover to bare area from 1973 to

2013. More comprehensive descriptions of the change classes are further illustrated in the following graphs and table. A simple change image such as this, overlaid with other relevant data like the mining tenement boundaries, may be used by stakeholders and regulators to monitor mining activities within the mining tenements.

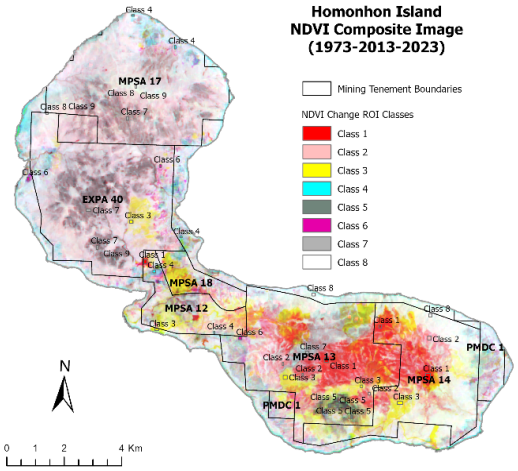

Figure 6. Composite NDVI image displayed in RGB (1973-2013-2023), overlaid with mining tenement boundaries and delineated class AOIs for the NDVI graphs.

The shape of the NDVI change graphs (Figure 7) for selected pixels corresponding to the identified but unlabelled classes are indicative of general land cover variations. These plots clearly show the transition of NDVI values over time, particularly for the significant decrease or increase in values. Caution must be applied when interpreting slight variations in the trend, since these may be artificially due to between-image discrepancies resulting from seasonality or sensor calibration differences.

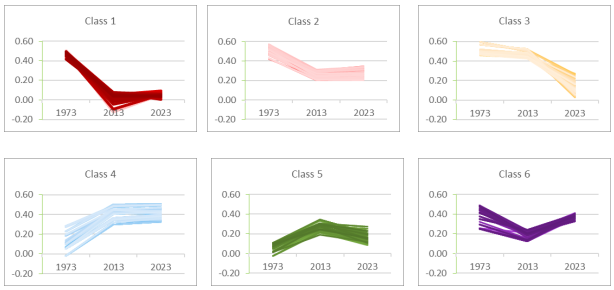

Figure 7. 3-year NDVI graphs for each change class.

These NDVI patterns for each identified class are quantified and summarized in Table 2, showing average NDVI values for each year and the inferred land cover change that occurred. These observed behavior from the NDVI graphs may be related to the mining progression in the area based on records and inferences. For instance, Class 1 may be related to the surge of clearing and mining activities in MPSA 12 approved in 2011, and in MPSA 13 and 14 both approved in 2009. The timeline and spatial distribution of this extensive landscape change coincides with the existence of the three MPSAs in the said areas. Class 2 (pink) shows a similar pattern, although with higher NDVI values for the latter dates, indicating a shift to sparse vegetation or grassland. Upon closer inspection, however, it appears that some Class 1 and Class 2 lines exhibit a slight increase in NDVI from 2013 to 2023, which may signify possible vegetation regrowth in some of the mined areas or may only be due to aforementioned image discrepancies. This theory should be further tested using more recent image years to check for a consistent and strong upward trend.

Class 3 (yellow) shows a drop in NDVI values from 2013 to 2023, with only a slight decrease from 1973 to 2013, implying that the shift from vegetation to bare soil may have started around 2013. The areas exhibiting this change class are along the fringes of the initial changes under Class 1 and 2, suggesting that the Class 3 areas are expansion areas for the mining activities within the same three MPSAs. Class 4 exhibits an opposite trend compared to Class 3, with NDVI values increasing from 1973 to 2013, signifying vegetation growth between the two years. A similar shape can be observed for Class 5, but with lower NDVI values between 0.1 to 0.3 corresponding to bare soil to sparse grassy areas. The temporal pattern of Class 6, exhibiting a significant dip in 2013 and almost equivalent values for 1973 and 2023, appears to be due to a seasonal land use such as agricultural activities. Class 7 and 8, not shown as graphs, only show almost stable NDVI behavior indicating zero to minimal change in the land cover. The lower NDVI range for Class 7 implies stable grasslands, while Class 8 implies relatively stable, moderate tree vegetation.

Class	NDVI trendline behavior	Land cover change	Ave NDVI 1973, 2013, 2023
1	Down 1973 to 2013	Tree to Bare	0.47, 0.03, 0.05
2	Slight down 1973 to 2013	Tree to Grass	0.51, 0.25, 0.26
3	Down 2013 to 2023	Tree to Bare	0.51, 0.46, 0.11
4	Up 1973 to 2013	Bare to tree	0.11, 0.40, 0.42
5	Slight up 1973 to 2013	Bare to grass	0.07, 0.27, 0.16
6	Down then upward	Seasonal crop	0.41, 0.19, 0.37
7	Almost horizontal	Stable grass	0.22, 0.27, 0.27
8	Almost horizontal	Stable tree	0.55, 0.51, 0.48

Table 2. Summary of NDVI trend descriptions per class.

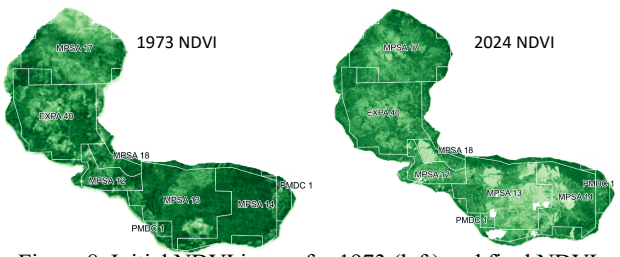

Figure 8. Initial NDVI image for 1973 (left) and final NDVI image for 2024 (right) signifying change in vegetation cover.

The more comprehensive and detailed analysis of NDVI variation using GEE resulted in 17 NDVI maps for each image scene. The comparison of the 1973 and 2024 NDVI images (Figure 8) reveal that the island initially had generally high NDVI shown as dark green areas, indicating good vegetation or forest cover. However, the latest result in 2024 exhibited a growing area with NDVI values close to zero, indicating vegetation loss, particularly in the southwestern portion. This spatial trend coincides with the location of mining tenements approved during the 1990s, suggesting a potential link of the vegetation decline.

The NDVI change plot for the fine-scale change analysis (Figure 9) further illustrates the abrupt drop in NDVI values years after the onset of mining activities. The drop in NDVI values around the mid-1990s in the 17-year analysis was not captured in the 3-year analysis. It is interesting to note that based on this more complete timeline, the dramatic decrease in NDVI actually began around 1995. Although some reports have mentioned the

degradation of forests around the 1990s due to massive open pit mining, there are no publicly available official reports regarding this issue. Based on reports and the MGB mining tenement map, the earliest mining permits that are active were approved in 2009 and 2011. This is contrary to the results showing a severe drop in NDVI values in the mid-1990s. It is possible that there were mining permits issued in the 1980s and actively operational in the 1990s causing the vegetation loss indicated by the significant NDVI decrease. This explanation for this alarming occurrence that is glaringly visible from the NDVI results warrants further validation in future studies.

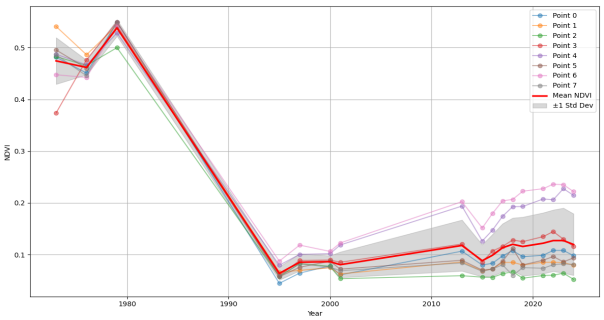

Figure 9. Temporal plots of the 17-year NDVI change.

It is also noteworthy that a significant drop in NDVI was observed in the 2015 result, closely following the abrupt decline seen in the 2013 result for the 3-year analysis. This decline aligns with data from the DENR-MGB indicating that Techiron Resources, Inc. began its mining operations on Homonhon Island in the same year. The areas affected include the barangays of Cagusu-an, Pagbabangnan, Casuguran, and neighboring communities such as Canawayon and Culasi – locations that also correspond to zones identified as rich in chromite, nickel, and other associated mineral deposits. The timing and spatial alignment suggest a strong correlation between the onset of mining activities and the observed vegetation degradation. There appears to be some revegetation for some of the point locations plotted, as indicated by the generally upward trend from the mid-1990s to the post-2020s. This occurrence is similar to the Class 1 and Class 2 trend in the 3-year analysis, and thus need to be further validated to separate it from artificial increase due to seasonality and different Landsat missions.

Using linear regression (Figure 10), the NDVI trend analysis revealed a mean slope of -0.0014 per year, indicating consistent annual decline in vegetation cover across the study area. Slope values ranging from -0.0128 to 0.0113 per year and a standard deviation of 0.0028 per year, reflect spatial variability in vegetation dynamics. The coefficient of determination (R^2) had a mean value of 0.24 and a standard deviation of 0.23, suggesting predominantly weak to moderate fit, although certain localized areas exhibited strong linear relationships. The overall negative slope points to vegetation decline that may be attributed to intensive land-use changes, particularly mining activities within the MPSAs, typically resulting in large-scale forest clearing, soil disturbance, and delayed or limited vegetation recovery. The relatively low R^2 values may be due to factors such as sudden expansion of mining areas, sporadic vegetation growth, or seasonal variations, which caused the non-linearity.

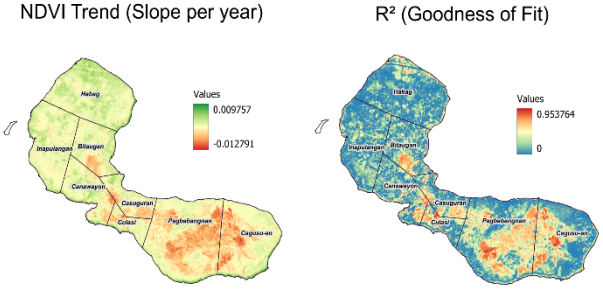

Figure 10. NDVI slope (left) and coefficient of determination (R^2) analysis (right) across the study period.

The accuracy assessment for the 31 August 2023 NDVI image using the 2,800 validation points resulted to an overall accuracy of 86.75% and kappa statistic of 79.75%. For the 2024 NDVI image under the 17-year analysis, 100 validation points were excluded since they fell within NoData pixels. The resulting overall accuracy and kappa statistic were 84.67% and 76.43%, respectively. In both NDVI results, the most confusion was encountered between grass and tree pixels, most probably due to the transitions between vegetation classes. The producer's accuracies for the grass class were at 55-57% for the two dates. On the other hand, bare areas and tree cover had high producer's accuracies at 92-100%.

3.1.2 Spatiotemporal Impact Analysis: The NDVI change results were overlaid with the mining tenement polygons to determine which of the landscape changes are found within the mined areas. Additional layers, such as building footprints as proxy for human population and biodiversity survey locations, were also included. The spatial relationships resulting from the overlay were used in explaining the temporal change behavior and its possible implications on the population and surrounding environment. Out of 1,957 building features from OSM, a total of 545 were found within or intersected the mining tenement boundaries classified as MPSA, PMDC, or EXPA. The rest of the building features are within 1 km from the tenement boundaries based on the Distance Accumulation proximity analysis. Even upon visual inspection of the overlay map (Figure 11), it is evident that most of the building clusters along the coastline are adjacent to the mining tenement boundaries. Although the exact differentiation between local community buildings and buildings for mining activities was not done, it can be assumed that the building clusters along the coastline are local communities and not mining camps. The close proximity of mining tenement boundaries with the local community clusters, and even complete containment in the case of MPSA 17, implies that local communities are most likely affected by mining activities.

The most obvious manifestation of open pit mining is the clearing of vegetated areas, including forest lands. Since the law does not restrict mining tenements from forestlands, it is important to assess how mining activities impact the natural environment in terms of forest cover loss. Using the raster calculator, NDVI maps from the earliest (1973) and latest (2024) years were subtracted to assess changes in the spatial distribution of vegetated areas in the island (Figure 11). Positive values indicate increased vegetation density or health, while negative values suggest vegetation loss or degradation. Approximately 56% of the study area, excluding the masked cloud and shadow areas, exhibited a decline in NDVI. In contrast, areas that experienced an increase or stable NDVI amounted to 24% of the total usable image area.

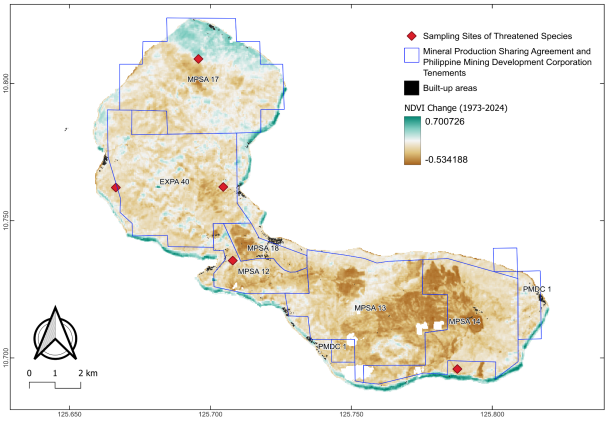

Figure 11. 17-year NDVI change map, overlaid with mining tenements, OSM buildings, and species sampling site locations.

Forest loss is closely related to biodiversity loss, not only for plant species, but also for faunal species that are dependent on forests for habitat and food. The number of threatened flora species taken from Romeroso et al. (2024) are listed according to mining tenement in Table 3. This summarized list shows that two of the five MPSAs and the EXPA site have threatened plant species that need to be protected. Since surface mining involves extensive clearing of vegetated areas, these important species are in danger of being lost if appropriate conservation measures are not implemented. Based on the IUCN Redlist of Threatened Species polygons, there are 19 records of threatened species overlapping with Homonhon Island, including the endangered mangrove species Camptostemon philippinensis. The IUCN known range polygons, however, need to be further validated for actual current presence and to determine whether the species overlap with the mining tenements.

Mining Tenement	IUCN 2023			DAO 2017-11		
	VU	EN	CR	VU	EN	CR
MPSA 12	4	2	-	4	1	4
MPSA 17	2	-	-	7	3	2
EXPA 40	1	3	-	3	1	4

Table 3. Summarize threatened species in mining tenements.

The mean NDVI over the 17-year time series of Landsat images spanning more than 50 years emphasizes the fact that vegetation cover has undergone significant changes, with evident signs of degradation in areas subjected to mining activities. The values from these years reveal a consistent decline in vegetation, especially in the southern part of Homonhon Island. Notably, higher levels of degradation appear in upland areas compared to the lowlands. These high elevation areas were once densely vegetated, exhibiting higher baseline NDVI. With the onset of mining activities resulting in clearing of forests, the drop in NDVI was significantly more glaring. In contrast, lowland areas that may have been less dense initially, do not show very drastic NDVI decline despite disturbance. This observation suggests that elevation and the initial state of vegetation may influence the severity of the NDVI change. In terms of monitoring, this highlights the importance of examining spatial patterns to better understand which areas are most affected and where conservation or restoration efforts should be prioritized.

4. Conclusions and Recommendations

Mining can lead to rapid landscape transformations, resulting in habitat degradation and biodiversity loss. Urban and economic development can occur in areas with high biodiversity; thus, proper conservation planning plays a key role in sustaining the balance. Since the Philippine Mining Act 1995 does not prohibit mining tenements from overlapping with local community areas and forestlands, it is crucial to ensure that harmful effects to the human population and biodiversity are prevented. Applying spatiotemporal approaches enables systematic assessment and monitoring of rapidly transforming landscapes, such as mining areas, thereby informing strategies for sustainable management.

The entire life cycle of a mining site, from planning to rehabilitation, may be analyzed using geospatial technologies, such as remote sensing and GIS. NDVI as a simple but effective tool for environmental monitoring was highlighted in various aspects in this study. Aside from its capability to discriminate between vegetated and bare areas, it was also utilized to analyze specific land cover transitions that occurred in the area. The generation of yearly NDVI maps and combining them to detect change can produce useful results for stakeholders in order to make appropriate and timely actions. Moreover, the use of spatial analysis to identify relationships and patterns gives a comprehensive view of the possible impacts of mining activities to the surrounding environment and local community.

This study's methodology can be an effective tool for monitoring and rehabilitating Homonhon and other mining sites. The 3-year analysis provided broader spatial coverage, while the 17-year analysis offered finer temporal detail. Results show that over the past 50 years, Homonhon has faced extensive vegetation loss, residential encroachment, and threats to biodiversity. With over 80% of the island covered by active and expanding mining tenements valid for up to two more decades, strict monitoring is crucial. Future refinements may include focusing spatial analysis on local residences and community structures, integrating field-validated species distribution data for more precise biodiversity assessments, and using complementary indices such as soil quality to strengthen degradation analysis. These enhancements will allow for a more reliable evaluation of mining's socio-ecological impacts.

References

Chen, F., Lou, S., Fan, Q., Wang, C., Claverie, M., Wang, C., Li, J., 2019. Normalized difference vegetation index continuity of the Landsat 4-5 MSS and TM: Investigations based on simulation. *Remote Sens,* 11(1681). doi.org/10.3390/rs11141681

Chugh, Y.P., Schladweiler, B.K., Skilbred, C., 2023. Sustainable and responsible mining through sound mine closure. *Int J Coal Sci Technol*, 10(14). doi.org/10.1007/s40789-023-00572-x.

Conde, M. and Le Billon, P., 2017: Why do some communities resist mining projects while others do not? *The Extractive Industries and Society*, 4(3), 681-697. doi.org/10.1016/j.exis.2017.04.009.

Dehkordi, M.M., Nodeh, Z.P., Dehkordi, K.S., Salmanvandi, H., Khorjestan, R.R., Ghaffarzadeh, M., 2024. Soil, air, and water pollution from mining and industrial activities: Sources of pollution, environmental impacts, and prevention and control methods. *Results in Engineering*, 23, 102729, doi.org/10.1016/j.rineng.2024.102729.

Electronics Watch, 2022. Human rights and environmental impact of nickel mining at Rio Tuba. Amsterdam, The Netherlands.

Genchi, G., Carocci, A., Lauria, G., Sinicropi, M.S., Catalano, A., 2020. Nickel: Human health and environmental toxicology. *Int. J. Environ. Res. Public Health* 17 (679), doi.org/10.3390/ijerph17030679.

Gupta, N., Yadav, K.K., Kumar, V., Kumar, S., Chadd, R.P., Kumar, A., 2019: Trace elements in soil-vegetables interface: Translocation, bioaccumulation, toxicity and amelioration - A review. *Science of The Total Environment* 651 (2), 2927-2942, doi.org/10.1016/j.scitotenv.2018.10.047.

Hengkai, L., Feng, X., Qin, L., 2020. Remote sensing monitoring of land damage and restoration in rare earth mining areas in 6 counties in southern Jiangxi based on multisource sequential images. Journal of Environmental Management, 267(110653). doi.org/10.1016/j.jenvman.2020.110653.

Jitar, O., Teodosiu, C., Oros, A., Plavan, G., Nicoara, M., 2015: Bioaccumulation of heavy metals in marine organisms from the Romanian sector of the Black Sea. *New Biotechnology* 32 (3), 369-378, doi.org/10.1016/j.nbt.2014.11.004.

Larsen, F.W., Turner, W.R., Brooks, T.M., 2012. Conserving Critical Sites for Biodiversity Provides Disproportionate Benefits to People. *PLoS ONE* 7(5): e36971. doi.org/10.1371/journal.pone.0036971.

Li, J., Zipper, C.E., Donovan, P.F., Wynne, R.H, Oliphant, A.J., 2015. Reconstructing disturbance history for an intensively mined region by time-series analysis of Landsat imagery. *Environ Monit Assess*, 187(557), doi.org/10.1007/s10661-015-4766-1.

Marticio, M.T., 2021. Endangered PH cockatoo spotted in Eastern Samar. *Manila Bulletin*. Retrieved June 12, 2025, from https://mb.com.ph/2021/5/26/endangered-ph-cockatoo-spotted-in-eastern-samar.

Markogianni, V., Dimitriou, E., 2016: Landuse and NDVI change analysis of Sperchios river basin (Greece) with different spatial resolution sensor data by Landsat/MSS/TM and OLI. *Desalination and Water Treatment*, 57(60), 29092–29103, doi.org/10.1080/19443994.2016.1188734.

Mines and Geosciences Bureau (MGB), 2025. Retrieved May 14, 2025, from https://mgb.gov.ph/images/Mineral_Statistics/2024/MINERALS_INDUSTRY_AT_A_GLANCE_Updated_11_April_2025.pdf

Murguía, D.I., Bringezu, S., Schaldach, R., 2016: Global direct pressures on biodiversity by large-scale metal mining: Spatial distribution and implications for conservation, *Journal of Environmental Management*, 180, 409-420, doi.org/10.1016/j.jenvman.2016.05.040.

Peck, P., Balkau, F., Bogdanovic, J., Sevaldsen, P., Skaalvik, J.F., Simonett, O., Thorsen, T.A., Kadyrzhanova, I., Svedberg, P., Daussa, R., 2005. Mining for Closure: policies, practices and guidelines for sustainable mining practices and closure of mines. UNEP, UNDP, OSCE, NATO ISBN: 82-7701-037-0.

Pettorelli, N., 2013. The Normalized Difference Vegetation Index. *Oxford*, 2013; online edn, Oxford Academic, 8 May 2015. doi.org/10.1093/acprof:osobl/9780199693160.001.0001.

Prasad, S., Yadav, K.K., Kumar, S., Gupta, N., Cabral-Pinto, M.M.S., Rezania, S., Radwan, N., 2021. Chromium contamination and effect on environmental health and its remediation: A sustainable approaches. *Journal of Environmental Management* 285(112174). doi.org/10.1016/j.jenvman.2021.112174.

Ramadhan, C., Dina, R., Nurjani, E., 2023. Spatial and temporal based deforestation proclivity analysis on flood events with applying watershed scale (case study: Lasolo watershed in Southeast Sulawesi, Central Sulawesi, and South Sulawesi, Indonesia), *International Journal of Disaster Risk Reduction*, 93(103745), doi.org/10.1016/j.ijdrr.2023.103745.

Reichl, C. and Schatz, M., 2022. World Mining Data 2022, Vol. 37. Federal Ministry of Agriculture, Regions and Tourism, Vienna. ISBN 978-3-901074-52-3.

Romeroso, R.B., Ordas, J.A.D., Tandang, D.N., Navarrete, I.A., Moran, C.B., 2024. Floral composition and diversity of ultramafic forests in Homonhon Island, Eastern Samar, Philippines, *Journal of Asia-Pacific Biodiversity*, 17 (2024) 7e20. doi.org/10.1016/j.japb.2023.10.001.

Schoderer, M. and Ott, M., 2022. Contested water- and miningscapes – Explaining the high intensity of water and mining conflicts in a meta-study. *World Development* 154 (2022) 105888. doi.org/10.1016/j.worlddev.2022.105888.

Secretariat of the Convention on Biological Diversity, 2005. Handbook of the Convention on Biological Diversity Including its Cartagena Protocol on Biosafety, 3rd edition, Montreal, Canada.

Senouci, O., 2020. Mining: A Key Human Cause of Landslides. *International Research Journal of Engineering and Technology (IRJET)*, 7(4).

Sonter, L.J., Ali, S.H., Watson, J.E.M, 2018. Mining and biodiversity: key issues and research needs in conservation science. *Proc Biol Sci.* 285(1892):20181926. doi.org/10.1098/rspb.2018.1926.

Stanimirova, R., Harris, N., Reytar, K., Wang, K., Barbanell, M., 2024. Mining Is Increasingly Pushing into Critical Rainforests and Protected Areas. World Resources Institute. Retrieved May 28, 2025, from https://www.wri.org/insights/how-mining-impacts-forests.

Williams, D., 2016. Chapter 37 - Tailings Storage Facilities, Adams, M.D. (ed.), Gold Ore Processing (2nd ed.), *Elsevier*, 663-676, doi.org/10.1016/B978-0-444-63658-4.00037-2.

Zhang, W., Dulloo, E., Kennedy, G., Bailey, A., Sandhu, H., Nkonya, E., 2019: Chapter 8 - Biodiversity and Ecosystem Services. *Sustainable Food and Agriculture*, Academic Press, Campanhola, C. and Pandey, S. 137-152, doi.org/10.1016/B978-0-12-812134-4.00008-X.

Zhao, C., Wu, Z., Qin, Q., Ye, X., 2022. A framework of generating land surface reflectance of China early Landsat MSS images by visibility data and its evaluation. *Remote Sensing*, 14(8), 1802. doi.org/10.3390/rs14081802.